

## Supporting Information

### The role of dopant ions on charge injection and transport in electrochemically doped quantum dot films

*Solrun Gudjonsdottir<sup>1</sup>, Ward van der Stam<sup>1</sup>, Nicholas Kirkwood<sup>1</sup>, Wiel H. Evers<sup>1,2</sup>, Arjan J. Houtepen<sup>1\*</sup>*

<sup>1</sup>Chemical Engineering, Optoelectronic Materials, Delft University of Technology, Van der Maasweg 9, 2629 HZ Delft, The Netherlands

<sup>2</sup>Kavli Institute of Nanoscience, Delft University of Technology, Van der Maasweg 9, 2629 HZ Delft, The Netherlands

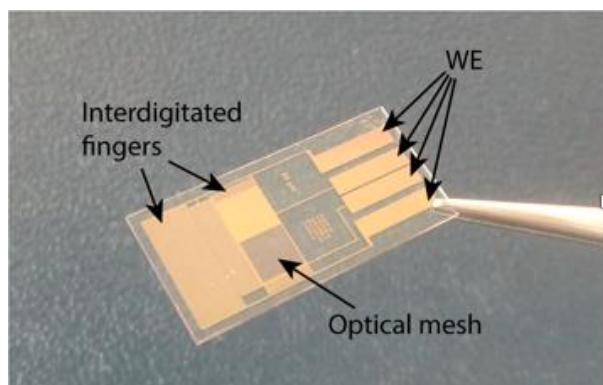


**Figure S1.** Home-built interdigitated electrode. The electrode is a glass substrate coated with four separate gold working electrodes prepared in house via optical lithography. These four gold working electrodes provide five source-drain gaps of different sensitivities. The electrode includes a gold mesh for optical measurements and a gold square for reflection measurements.

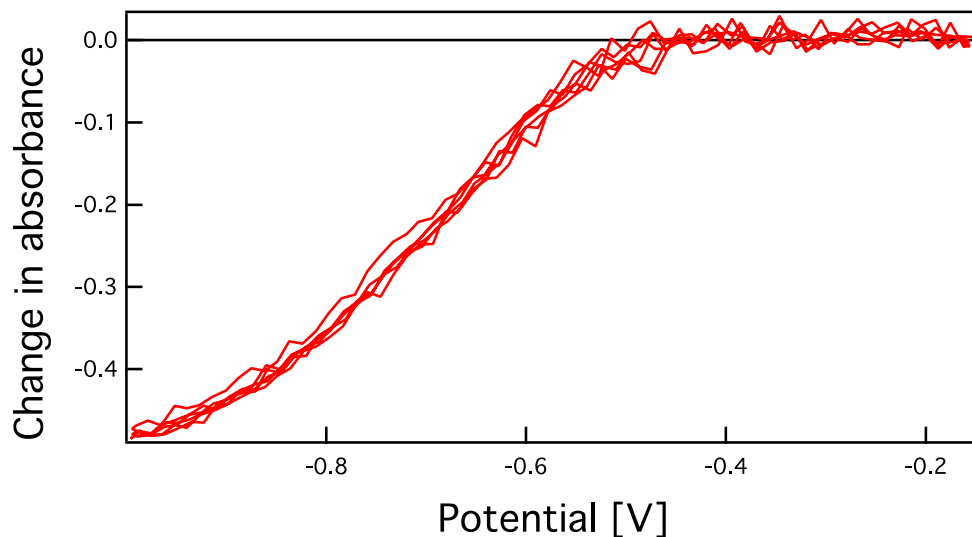


**Figure S2.** Change in absorbance during a CV scan for a ZnO QD film immersed in 0.1 M LiClO<sub>4</sub> acetonitrile electrolyte solution. This is at the 1s peak of the ZnO QD film. The scan is in negative direction and repeated three times.

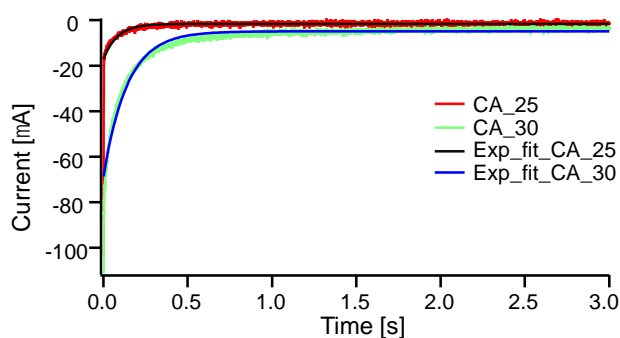


**Figure S3.** Exponential fit for charging currents. An exponential fit suits the curves well after the initial drop of the current.

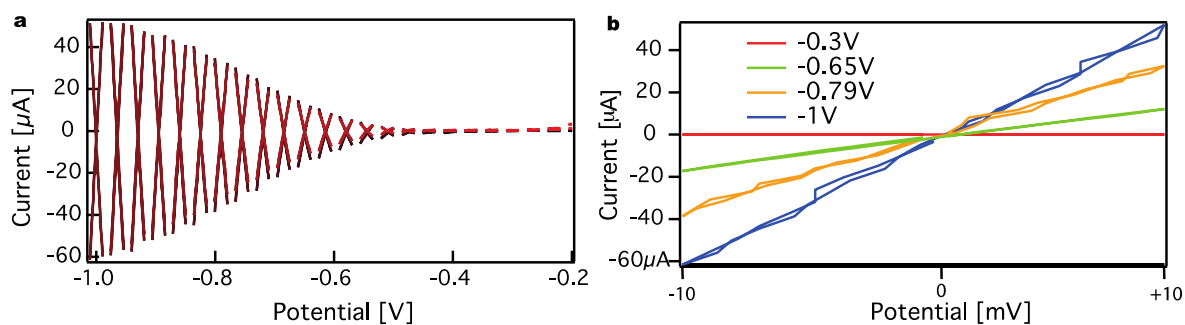


**Figure S4.** Source-drain electron conductivity measurements. (a) The CVs from both WE1 and WE2. WE1 is scanned  $\pm 10$  mV around the potential of WE2 and a potential step of 35 mV is taken between each measurement. (b) The source-drain output for WE2 for picked potentials. The slope gives the conductance.

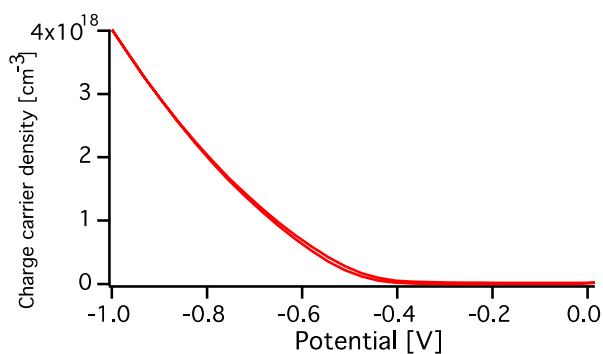


**Figure S5.** Charge carrier density calculated from the differential capacitance measurements.

#### *Randles-Sevcik equation for porous QD films*

We use the Randles-Sevcik equation to calculate the diffusion coefficient for different electrolyte cations. This can be rationalized by considering that the concentration profiles for diffusion of excess  $\text{Li}^+$  is similar compared to a concentration profile of diffusion of reactant from a bulk solution (Fig. S5). When the QD film is immersed in the electrolyte solution, some ions diffuse into the voids of the film. However, the concentration of ions in the film is not necessarily the same as in the bulk,  $C^*$ , as it may be more difficult for the ions to diffuse into the voids than out of them. Therefore, the concentrations are related via the partition coefficient,  $\gamma$  (Fig. S5). The potential of the working electrode can be changed compared to a reference electrode, and if a negative enough potential is applied, electrons can flow into the QD film. To compensate for the charge, cations flow into the voids of the film. As more electrons are injected, more cations are required to compensate the injected charge and the concentration of excess cations (cations that do not participate to neutralize the film) decreases in the film. This process will start at the electrode surface resulting in a concentration profile such as is shown in Figure S5. The diffusion current,  $i$ , can be related to the diffusion coefficient,  $D$ , and the ion concentration,  $c$ , by equation S1:

$$i = eD \frac{dc}{dx} \quad (\text{S1})$$

where  $x$  is the distance from the working electrode. The concentration gradient, and hence the diffusion current, will decrease with time. The solution to this problem for ions in solution in contact with a flat electrode is the Randles-Sevcik equation. The ion diffusion in a porous film can be expected to be similar.

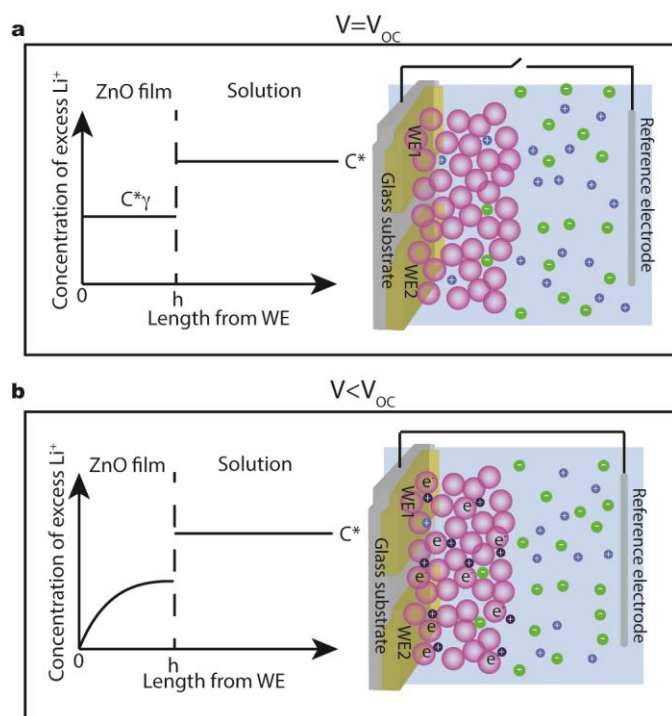


**Figure S6.** Schematic of the QD film after immersion in the electrolyte. (a) The concentration of  $\text{Li}^+$  is the same throughout the QD film.  $h$  stands for the film height,  $C^*$  for the bulk concentration and  $\gamma$  is the partition coefficient. (b) The concentration of excess  $\text{Li}^+$  decreases in the film as  $\text{Li}^+$  neutralizes injected charge and new  $\text{Li}^+$  need to diffuse from the bulk solution.

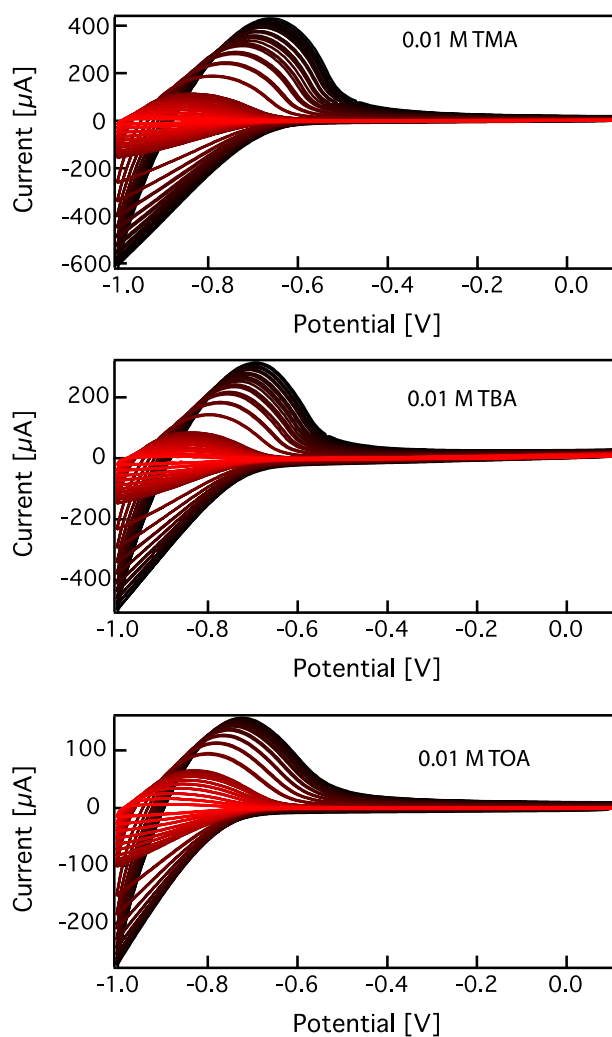


**Figure S7.** A magnification of the CVs in Figure 5 in the manuscript. CVs taken at different scan rates for 0.01 M TMA<sup>+</sup>, TBA<sup>+</sup> or TOA<sup>+</sup> in acetonitrile electrolyte solution. The scans have negative direction and are repeated three times for every scan rate.

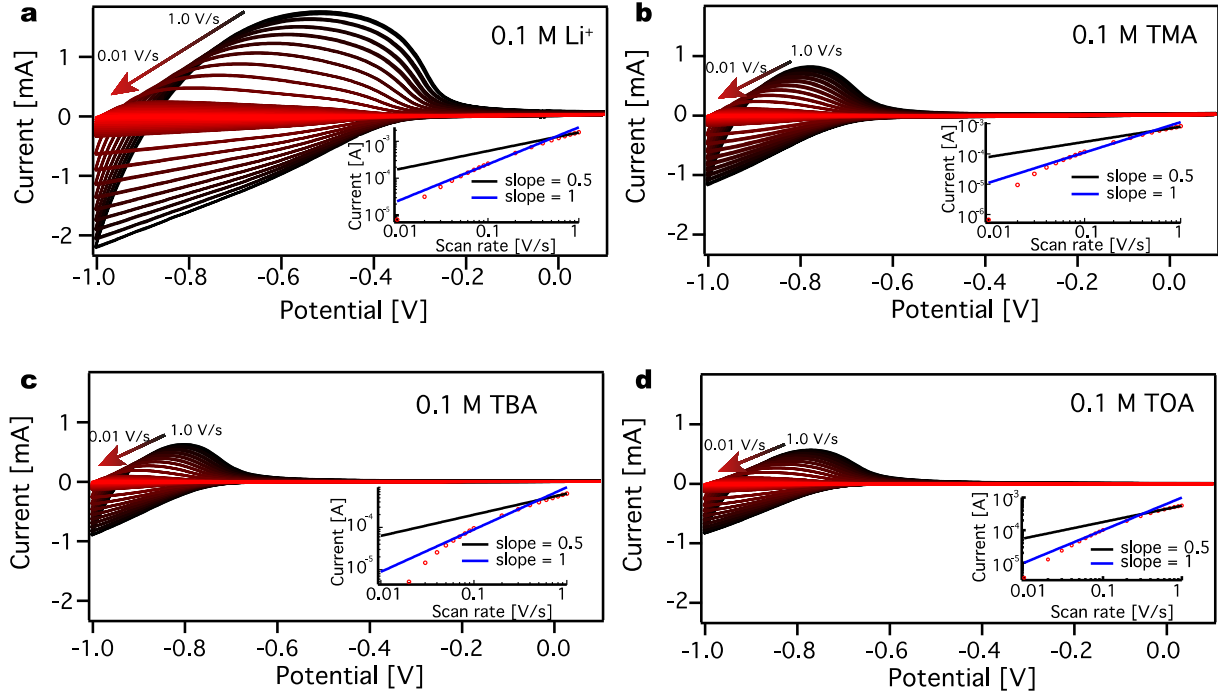


**Figure S8.** CVs for ZnO QD films immersed in (a) 0.1 M LiClO<sub>4</sub> acetonitrile electrolyte solution, (b) 0.1 M tetramethylammonium hexafluorophosphate (CH<sub>3</sub>)<sub>4</sub>N(PF<sub>6</sub>) acetonitrile electrolyte solution, (c) 0.1 M tetrabutylammonium perchlorate (CH<sub>3</sub>(CH<sub>2</sub>)<sub>3</sub>)<sub>4</sub>N(ClO<sub>4</sub>) acetonitrile electrolyte solution and (d) 0.1 M tetrabutylammonium tetrafluoroborate (CH<sub>3</sub>(CH<sub>2</sub>)<sub>7</sub>)<sub>4</sub>N(BF<sub>4</sub>) acetonitrile electrolyte solution. The scan rates are between 0.01 V/s to 1.0 V/s, the scan starts in negative direction and is repeated three times for each scan rate. Each panel includes a log-log plot of the peak current versus scan rate. The slope in the insets is given by  $\frac{d \log I}{d \log \nu}$  where  $I$  is the current and  $\nu$  is the scan rate.

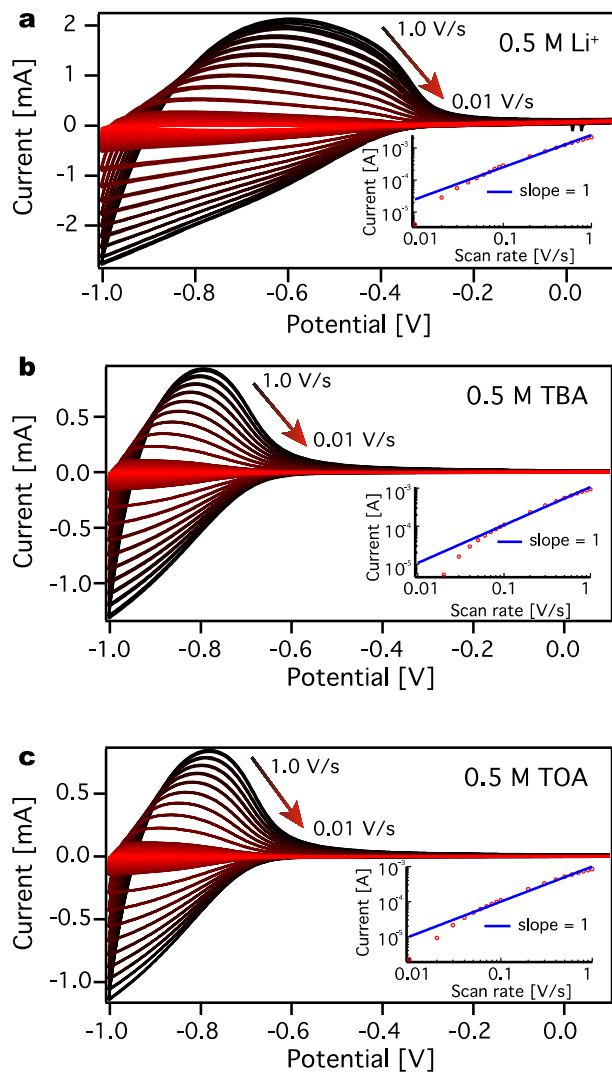


**Figure S9.** CVs for ZnO QD films immersed in (a) 0.5 M LiClO<sub>4</sub> acetonitrile electrolyte solution, (b) 0.5 M tetrabutylammonium perchlorate (CH<sub>3</sub>(CH<sub>2</sub>)<sub>3</sub>)<sub>4</sub>N(ClO<sub>4</sub>) acetonitrile electrolyte solution and (c) 0.5 M tetraoctylammonium tetrafluoroborate (CH<sub>3</sub>(CH<sub>2</sub>)<sub>7</sub>)<sub>4</sub>N(BF<sub>4</sub>) acetonitrile electrolyte solution. The scan rates are between 0.01 V/s to 1.0 V/s, the scan starts in negative direction and is repeated three times for each scan rate. Each panel includes a log-log plot of the peak current versus scan rate. The slope in the insets is given by  $\frac{d \log I}{d \log v}$  where  $I$  is the current and  $v$  is the scan rate.

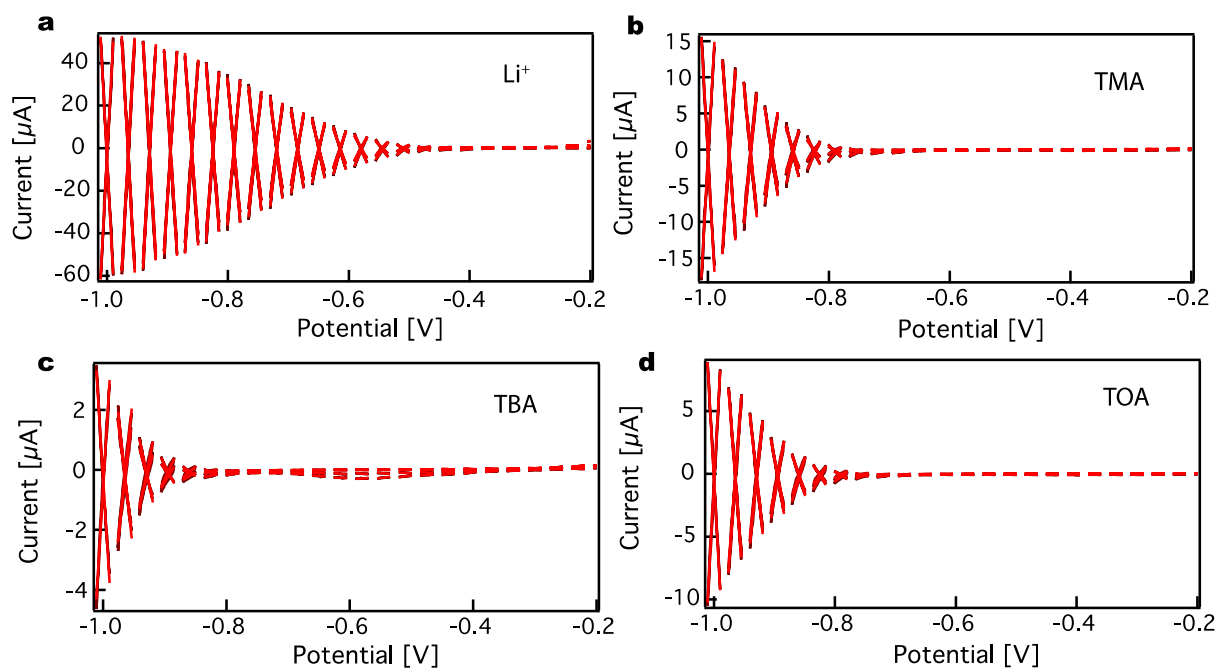


**Figure S10.** Source-drain electronic conduction measurements in (a) 0.1 M  $\text{LiClO}_4$  acetonitrile electrolyte solution, (b) 0.1 M tetramethylammonium hexafluorophosphate  $(\text{CH}_3)_4\text{N}(\text{PF}_6)$  acetonitrile electrolyte solution, (c) 0.1 M tetrabutylammonium perchlorate  $(\text{CH}_3(\text{CH}_2)_3)_4\text{N}(\text{ClO}_4)$  acetonitrile electrolyte solution and (d) 0.1 M tetraoctylammonium tetrafluoroborate  $(\text{CH}_3(\text{CH}_2)_7)_4\text{N}(\text{BF}_4)$  acetonitrile electrolyte solution. The CVs are both from WE1 and WE2. WE1 is scanned  $\pm 10$  mV around the potential of WE2 and a potential step of 35 mV is taken between each measurement.

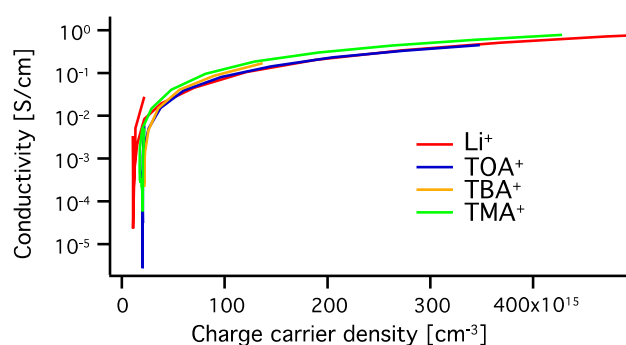


**Figure S11.** Calculated conductivity vs. the charge carrier density for 0.1 M acetonitrile electrolyte solution. The used electrolytes are lithium perchlorate, tetramethylammonium hexafluorophosphate, tetrabutylammonium perchlorate and tetraoctylammonium tetrafluoroborate.



### *Determination of the threshold potential*

In order to determine the threshold potential, the potential of the conductivity for each cation was shifted compared to the potential of the conductivity of  $\text{Li}^+$ . That is, the threshold potential was determined by finding the minimum of the following equation:

$$\sigma_{\text{Li}^+} - \sigma_{\text{cat}^+}(V - V_{th}) \quad (\text{S2})$$

Where  $\sigma_{\text{Li}^+}$  is the conductivity when  $\text{Li}^+$  is the electrolyte cation,  $\sigma_{\text{cat}^+}$  is the conductivity when other ions than  $\text{Li}^+$  are used,  $V$  is the potential and  $V_{th}$  is the threshold potential.